

Hairy black holes and holographic heat engine

H. Ghaffarnejad ^{† 1} E. Yaraie ^{†2} M. Farsam ^{†3} K. Bamba^{‡ 4}

[†]*Faculty of Physics, Semnan University, P.C. 35131-19111, Semnan, Iran*

[‡]*Division of Human Support System, Faculty of Symbiotic Systems
Science, Fukushima University, Fukushima 960-1296, Japan*

Abstract

By considering AdS charged black hole in the context of extended thermodynamic as the working substance we use it as a heat engine. We investigate the effect of hairy charge on the evolution of efficiency and Carnot efficiency along with electric charge. Because of interesting thermodynamic behavior of hairy black holes it would be natural to know their effects when we use black hole as a heat engine. We show that the hairy charge increases the efficiency, and so maximum temperature would be happened for bigger Maxwell charge when this hairy charge grows. For the fixed electric charges, the efficiency has a minimum value. In fact all critical points describe physical states except when the charge removed. If the electric charge takes a zero value then the hairy charge must be negative. We also seek behavior of the system for large charges which is provided a model with low-temperature thermodynamics.

1 Introduction

Quantum field theory (QFT) propagated in curved spacetimes was studied from decade of 1970 where there is found a relationship between geometrical and thermodynamical features of black hole, for instance one can obtain a relation between the event horizon surface and its entropy. In fact it is a relation between the surface gravity and the temperature [1,2]. This implicated a basic connection among quantum theories, thermodynamics and gravity that led to the birth of black hole thermodynamics laws. Hawking and Page showed in 1983, that there is a phase transition between a thermal

¹E-mail: hghafarnejad@semnan.ac.ir

²E-mail: eyaraie@semnan.ac.ir

³E-mail: mhdffarsam@semnan.ac.ir

⁴E-mail: bamba@sss.fukushima-u.ac.jp

AdS spacetime and Schwarzschild black hole [3]. Chamblin *et al* tested in 1999, it for a charged AdS background in a canonical ensemble and obtained a phase transition between small and large black holes which is similar to the Van der Waals (VdW) phase transition [4,5]. Despite such results, due to the lack of a specific definition for the pressure and the volume of black holes this similarity is not perfect, while VdW fluid presents a first order kind of the phase transition in $P - V$ diagram.

In the other side Smarr relation [6,7] is not compatible with the black hole thermodynamics first law. After some pioneer works to promote the cosmological constant as a thermodynamic variable [8], Kastor in 2009 tried to resolve this problem by considering a variable cosmological parameter as pressure in the black hole thermodynamics first law [9]. He reached to generalized version of the first law of the black hole thermodynamics by considering the cosmological parameter as origin of the thermodynamic pressure which is conjugated quantity for the space time volume. By attention to these considerations one can see various behaviors and characteristics for black hole solutions similar to thermodynamic systems such as phase behaviors in gels and polymers or triple point in water. One of these aspects is behavior of heat engine which can be explored in black hole object.

From AdS/CFT duality, a gravity theory defined in AdS bulk spacetime corresponds to a conformal field theory defined on the boundary of AdS bulk spacetime with one dimension less. The cosmological constant will be related to a length scale ℓ in the d -dimensional bulk spacetime through $\Lambda = -(d-1)(d-2)/2\ell^2$. This length scale could be set by the number of coincident branes in which AdS/CFT correspondence becomes significant for its large numbers where the curvature of spacetime becomes small. In the field theory the number, N , determines degrees of freedom of boundary theory. So dynamical pressure in the bulk leads to dynamical N on the boundary corresponds to the changing IR fixed points of theory or triggering a RG flow on the boundary theory [10,11]. We can see from [12] when the black hole is considered as a working substance this relationship between P and N causes a correspondence between a heat engine in AdS and a cycle on the space of dual field theory side. Indeed the efficiency of heat engine might characterize a physical property for instance a near equilibrium expansion of an appropriate response function on the boundary [13]. In the case of hyperbolic black holes given by [14], heat flows and also work in field theory side are described as the difference in the entanglement entropy of two boundary theories which visit each other along the cycle. It must be also interesting to

study holographic heat engine at critical point at which its efficiency is very similar to Carnot engine's at finite power [15]. We can find a wide range of works in [14-30] at which the black hole is considered as a working substance. Pioneering works of Johnson for charged AdS black holes indicate that mechanical work can be extracted from heat energy via " PdV " term in the first law of thermodynamics. This is in contrary with Penrose process which leads to the extracting of energy from rotating black holes in both asymptotically AdS and flat spacetimes.

Of course it must be noted that some authors [31-33] found black hole metrics with conformal scalar hair in 4 dimensions in the case of vanishing cosmological constant but these scalar field configurations suffer from divergence at the horizon. There are not any black hole solutions for higher dimensions in this case [34,35]. Applying a non-vanishing cosmological constant, there are obtained some conformal hairy regular black hole solutions in 3 and 4 dimensions [36-40], but not for higher dimensions [41]. It is proved [42-44] that if the scalar field gets coupled conformally invariant to the higher order Euler densities then hairy black hole solution does exist for any dimension. Motivation of considering scalar fields has always been expected in theoretical physics and has played a fundamental role in the structure of string theory. Since the pure gravity is inconsistent at quantum mechanical level, so any theory comes to replace it must be included such additional scalar field due to its fundamental structure. In the other side scalar fields could be useful to understand black hole physics specially in higher dimensional black hole as a low energy effective string theory. Thermodynamics of the hairy black hole is studied in [45] at which phase transition including backreaction is solved explicitly. We consider the scalar hair field in a 5 dimensional RN black hole and study its holographic heat engine when the black hole behaves as a working substance. As a future work, we are interested to study thermodynamics of hairy black holes obtained from other alternative gravity models such as [46-52].

Layout of this work is as follows. In section 2 we set up hairy black hole solution and its thermodynamic aspects in AdS_5 space. We discuss relationship between the hairy and electric charges and seek the conditions for critical points. In section 3 we calculate the efficiency of the heat engine by regarding the effects of hairy and Maxwell charge. We find various areas of efficiency which is restricted due to the sign of Hawking temperature and the black hole entropy. We also study Carnot efficiency and its evolution with respect to the efficiency of heat engine. Finally, we can show that both of

these efficiencies approach to each other for large limit of hairy charge. At last section we present conclusion of this work and suggest some outlooks.

2 Thermodynamics of hairy black holes in a revisited AdS_5 space

To study hairy black holes in AdS_5 as a thermodynamic system we begin with the action as follows [44]:

$$I = \frac{1}{\kappa} \int d^5x \sqrt{-g} \left(R - 2\Lambda - \frac{1}{4} \mathcal{F}^2 + \kappa \mathcal{L}(\phi, \nabla\phi) \right) \quad (2.1)$$

where $\kappa = 16\pi G$ is the Newton's gravity coupling constant, $\mathcal{F}^2 = F_{\mu\nu}F^{\mu\nu}$ is the Lagrangian density of the electromagnetic fields and $\mathcal{L}(\phi, \nabla\phi)$ represents the Lagrangian of a conformally coupled real scalar field. In general, to express the conformal matter content, it is convenient to introduce the four-rank tensor

$$S_{\mu\nu}{}^{\gamma\delta} = \phi^2 R_{\mu\nu}{}^{\gamma\delta} - 12\delta_{[\mu}^{[\gamma}\delta_{\nu]}^{\delta]}\nabla_\rho\phi\nabla^\rho\phi - 48\phi\delta_{[\mu}^{[\gamma}\nabla_{\nu]}\nabla^{\delta]}\phi + 18\delta_{[\mu}^{[\gamma}\nabla_{\nu]}\phi\nabla^{\delta]}\phi. \quad (2.2)$$

In the latter case the Lagrangian density of a conformally coupled real scalar field in 5D is expressed by [44]

$$\mathcal{L}(\phi, \nabla\phi) = \phi^{15} (b_0 \mathcal{S}^{(0)} + b_1 \phi^{-8} \mathcal{S}^{(1)} + b_2 \phi^{-16} \mathcal{S}^{(2)}) \quad (2.3)$$

where

$$\begin{aligned} \mathcal{S}^{(0)} &= 1, \\ \mathcal{S}^{(1)} &= S \equiv g^{\mu\nu} S_{\mu\nu} = g^{\mu\nu} \delta_\sigma^\rho S_{\mu\rho\nu}^\sigma, \\ \mathcal{S}^{(2)} &= S_{\mu\nu\alpha\beta} S^{\mu\nu\alpha\beta} - 4S_{\mu\nu} S^{\mu\nu} + S^2, \end{aligned}$$

which contain higher order curvature couplings. In fact such couplings cause why this model happens to circumvent no-hair theorems [42]. We should notice that all terms of the Lagrangian (2.3) are well-behaved in the limit $\phi \rightarrow 0$ since the tensor field (2.2) is quadratic with respect to the scalar field

[42]. b_0 , b_1 and b_2 given in (2.2) are coupling constants. They are conformally invariant under the following Weyl rescaling transformations.

$$g_{\mu\nu} \rightarrow \Omega^2 g_{\mu\nu}, \quad \phi \rightarrow \Omega^{-1/3} \phi. \quad (2.4)$$

Applying (2.4), the tensor field (2.2) reads [44]

$$S_{\mu\nu}{}^{\gamma\delta} \rightarrow \Omega^{-8/3} S_{\mu\nu}{}^{\gamma\delta}. \quad (2.5)$$

Varying the action (2.1) with respect to the metric field $g_{\mu\nu}$ we can obtain the metric field equations

$$R_{\mu\nu} - \frac{1}{2} R g_{\mu\nu} + \Lambda g_{\mu\nu} = \kappa T_{\mu\nu}, \quad (2.6)$$

in which the energy momentum tensor is given by

$$T_{\mu}^{\nu} = \sum_{k=0}^2 \left(\frac{k! b_k}{2^{k+1}} \phi^{15-8k} \delta_{[\mu}^{\nu} \delta_{\rho_1}^{\lambda_1} \dots \delta_{\rho_{2k}}^{\lambda_{2k}]} \right) \times \left(S^{\rho_1 \rho_2}_{\lambda_1 \lambda_2} \dots S^{\rho_{2k-1} \rho_{2k}}_{\lambda_{2k-1} \lambda_{2k}} \right). \quad (2.7)$$

Giribet et al obtained a spherically symmetric static hairy black hole solution for (2.6) in 5 dimension as follows (see [44] and references therein).

$$ds^2 = -f(r) dt^2 + \frac{dr^2}{f(r)} + r^2 d\Omega_3^2 \quad (2.8)$$

with

$$f(r) = 1 - \frac{m}{r^2} - \frac{h}{r^3} + \frac{q^2}{r^4} - \frac{\Lambda}{6} r^2, \quad (2.9)$$

in which $d\Omega_3^2$ is the line element of the unit 3-sphere for which $\omega_3 = \int d\Omega_3^2 = 2\pi^2$. Here m is mass parameter of the system and q is electric charge parameter with Maxwell vector gauge potential $A_{\mu} = (\sqrt{3}e/r^2, 0, 0, 0)$. The coupling constant h given in the metric solution (2.9) represents hairy charge and is given by

$$h = \frac{64\pi G}{5} b_1 n^9, \quad n = \varepsilon \left(-\frac{18 b_1}{5 b_0} \right)^{1/6}, \quad (2.10)$$

with $\varepsilon = -1, 0, +1$ and extra condition $10b_0 b_2 = 9b_1^2$ which guarantees the metric solution (2.9) to have a black hole topology. Also the scalar field

configuration of this charge takes the form of $\phi(r) = \frac{n}{r^{1/3}}$. Thermodynamic quantities of this hairy black hole are given as follows [44].

$$Q = -\frac{\sqrt{3}\pi}{8}q \quad (2.11)$$

$$M = \frac{3\pi}{8}m = \frac{3\pi}{8} \left(r_+^2 - \frac{h}{r_+} + \frac{q^2}{r_+^2} + \frac{r_+^4}{\ell^2} \right), \quad (2.12)$$

$$S = \int_0^{r_+} \frac{1}{T} \left(\frac{\partial M}{\partial r_+} \right) dr_+ = 2\pi^2 \left(\frac{r_+^3}{4} - \frac{5}{8}h \right), \quad (2.13)$$

$$T(r_+) = \frac{1}{\pi\ell^2 r_+^4} \left(-\frac{q^2\ell^2}{2r_+} + \frac{h\ell^2}{4} + \frac{\ell^2}{2}r_+^3 + r_+^5 \right), \quad (2.14)$$

where the black hole event horizon r_+ is determined by solving the horizon equation $f(r_+) = 0$. The entropy computed in (2.13) differs from the standard Bekenstein-Hawking formula. In fact it accords to the Iyer-Wald's method [31, 33]. Since in the extended thermodynamics the black hole mass behaves as the enthalpy, so by regarding (2.11), (2.12), (2.13) and (2.14), we can reach to the first law of extended thermodynamics as follows.

$$dM = TdS + VdP + Kdh + \Phi dQ, \quad (2.15)$$

where the thermodynamic volume V is conjugate potential of the pressure in 5-dimensional space time given by $P = 3/4\pi\ell^2$. One can compute V and other conjugate potentials for hairy and electric charges indicated by K and Φ , respectively as follows:

$$V = \left(\frac{\partial M}{\partial P} \right)_{r_+} = \frac{\pi^2}{2} r_+^4, \quad (2.16)$$

$$K = \left(\frac{\partial M}{\partial h} \right)_{r_+} = \frac{\pi}{16\ell^2 r_+^5} (20r_+^6 + 4r_+^4\ell^2 + 5\ell^2 h r_+ - 10q^2\ell^2), \quad (2.17)$$

$$\Phi = \left(\frac{\partial M}{\partial Q} \right)_{r_+} = -\frac{2\sqrt{3}}{r_+^2}q. \quad (2.18)$$

The generalized Smarr relation regarding the scaling argument reads

$$2M = 3TS - 2VP + 3hK + 2\Phi Q. \quad (2.19)$$

Now we can obtain the equation of state for hairy black hole by using Hawking temperature (2.14) and definition of specific volume, $v = \frac{4}{3}r_+$ [34,55] such that,

$$P = \frac{T}{v} - \frac{2}{3\pi v^2} - \frac{64}{81} \frac{h}{\pi v^5} + \frac{512}{243} \frac{q^2}{\pi v^6}. \quad (2.20)$$

The critical points are obtained by solving the equations

$$\left. \frac{\partial P}{\partial v} \right|_{T=T_{cr}} = \left. \frac{\partial^2 P}{\partial v^2} \right|_{T=T_{cr}} = 0, \quad (2.21)$$

which in absence of the Maxwell field $q = 0$ they reduce to the solutions

$$v_{cr} = \frac{4}{3}(-5h)^{\frac{1}{3}}, \quad (2.22)$$

$$T_{cr} = -\frac{3}{20} \frac{(-5h)^{\frac{2}{3}}}{\pi h}, \quad (2.23)$$

$$P_{cr} = \frac{9}{200\pi} \left(\frac{-\sqrt{5}}{h} \right)^{\frac{2}{3}} \quad (2.24)$$

for which we must be choose $h < 0$ to have critical points with real values. In general for $q \neq 0$ one can obtain numerical solutions for (2.21) [32]. Regarding these results the situations are divided into two branches: If $h < 0$ then the critical points would be physical for all values of q , but if $h > 0$ then the equation of state admits a single inflection point. To have physical critical points the corresponding entropy should not to be negative for this inflection point. With numerical analysis, one can infer that all critical points defined on $h \approx 1.3375q^{3/2}$ are physical points with zero entropy. In the other side, all critical points under this curve in (h, q) parameter space are physical with positive entropy (see figure 3 in [32]).

3 Holography heat engines

In this section we study hairy black holes in AdS_5 spacetime which can be considered to be as the working substance of the heat engine. For this purpose we consider a rectangular cycle in $P - V$ diagram as shown in figure 1. As we explained in the introduction, variation of cosmological parameter (namely the pressure of the AdS spacetime) is viewed as the change of size of the AdS spacetime. All these changes cause to behave the curved spacetime as a

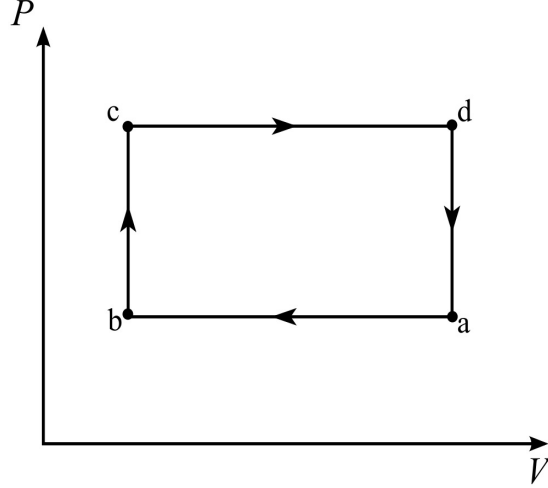


Figure 1: The heat engine cycle in $P - V$ plan for a thermodynamical system

thermodynamical system in which $P - V$ diagram is given in the figure 1. The cycle is made up of four processes: two constant volume processes (isocore) and two constant pressure processes (isobar). During this rectangular cycle, the system receives heat during $b \rightarrow c$ and $c \rightarrow d$, so the net amount of heat transferred to the system is $Q_H = Q_{b \rightarrow c} + Q_{c \rightarrow d}$. Then the system expels heat during $d \rightarrow a$ and $a \rightarrow b$. Because the process denoted by $b \rightarrow c$ takes place in constant volume, the amount of heat entered to the system would be equal to the changing in the internal energy of the system given by $\Delta U = Q_{bc} = C_v \Delta T_{b \rightarrow c}$. But since the volume and entropy of a black hole are both depend only on the radius of the horizon, we can conclude that the specific heat at constant volume vanishes so the system does not receive any heat during the $b \rightarrow c$ process. On the other side, the heat of the system absorbed during the isobaric process $c \rightarrow d$ can also be obtained from $Q_{cd} = C_P \Delta T_{b \rightarrow c}$. So the total heat entered into the system in this cycle is given by the following relation.

$$Q_H = \int_{T_c}^{T_d} C_P dT, \quad (3.1)$$

where the specific heat at constant pressure C_P is defined by

$$C_P = T \left(\frac{\partial S}{\partial T} \right)_P. \quad (3.2)$$

Applying metric potential (2.9) and horizon equation $f(r_+) = 0$ and thermodynamic quantities (2.11), (2.12), (2.13) and (2.14) one can show that the above heat capacity leads to the following form.

$$C_P = \frac{3(2PA^2\pi^2 + 12h\pi^4 B^{\frac{1}{3}} + 3(A\pi)^{\frac{7}{3}} - 48q^2\pi^5)}{16(240q^2\pi^5 + 2PA^2\pi^2 - 48h\pi^4 B^{\frac{1}{3}} - 3\pi(A\pi)^{\frac{4}{3}})}, \quad (3.3)$$

where $A = 20\pi^2 h + 16S$ and $B = 20\pi^3 h + 16S$. The inflow heat relation will be simplified by using (3.1) and (3.2) in the expansion process $c \rightarrow d$ if we hold all other quantities as constants. In the latter case we will have

$$Q_H = \int_{S_c}^{S_d} C_P \left(\frac{\partial T}{\partial S} \right)_P dS = \int_{S_c}^{S_d} T dS = \int_{M_c}^{M_d} dM = M_d - M_c. \quad (3.4)$$

For hairy AdS_5 black holes, from (2.12) we have

$$M_i = \frac{3\pi}{8} \left(r_{+i}^2 - \frac{h}{r_{+i}} + \frac{q^2}{r_{+i}^2} + \frac{4\pi}{3} P r_{+i}^4 \right), \quad (3.5)$$

where the event horizon radiuses $r_{+i} = \frac{1}{2\pi^{2/3}} A_i^{\frac{1}{3}}$ with $i = c, d$ and $A_i = 20\pi^2 h + 16S_i$ could be obtained from (2.13). So the net amount of heat which the system receives is

$$Q_H = M_d - M_c = \frac{3\pi}{8} \left(\frac{1}{4\pi^{4/3}} (A_d^{\frac{2}{3}} - A_c^{\frac{2}{3}}) - 2\pi^{2/3} h (A_d^{-\frac{1}{3}} - A_c^{-\frac{1}{3}}) + 4\pi^{4/3} q^2 (A_d^{-\frac{2}{3}} - A_c^{-\frac{2}{3}}) + \frac{P}{12\pi^{5/3}} (A_d^{\frac{4}{3}} - A_c^{\frac{4}{3}}) \right). \quad (3.6)$$

On the other side, the work performed by engine equals to the area enclosed by the cycle which is computed regarding figure 1 as follows:

$$W = (V_d - V_c)(P_c - P_b), \quad (3.7)$$

where subscripts denote to the points shown in the figure 1. So by attention to (2.16) the equation (3.7) reads

$$W = \frac{(A_d\pi)^{\frac{4}{3}} - (A_c\pi)^{\frac{4}{3}}}{32\pi^2} (P_c - P_b). \quad (3.8)$$

Finally we can demonstrate the performance of the heat engine by a thermal efficiency η as follows.

$$\eta = \frac{W}{Q_H}. \quad (3.9)$$

To investigate the effects of hairy and Maxwell charges on the performance of heat engine it would be useful to set one charge with unit and let the other one changes in the ranges with positive Hawking temperature. In figures 2.a and 2.b we show the maximum value of charge with a red spot after which Hawking temperature will be negative. As we can see from this maximum charge the thermal efficiency has also its maximum value.

In figure 2.a we plotted the heat engine efficiency versus the Maxwell charge by holding $P_c = 2$, $P_b = 1$, $S_c = 8$, $S_d = 10$ for various fixed hairy charge. The diagram shows that the efficiency grows by increasing the Maxwell charge for any fixed hairy black holes until it ceased at a maximum value of point (q_{max}, η_{max}) after which temperature would be negative.

Regarding numerical analysis which we pointed it out at end of the section 2 the critical points might be un-physical for $q \neq 0$ where $h > 0$ and the entropy reaches to some negative values. For example the blue line in figure 2.a is fixed at $h = 1$, so all physical critical points must be restricted by $q_{phys} \geq 0.6464862821$. The green line corresponds to AdS-RN black hole solution which is independent of the hairy charge [12]. In the latter case all points from $q = 0$ until a maximum value are physical. As we can see the existence of hairy charge increases the maximum point (q_{max}, η_{max}) . In other words the physical critical points admit synchronously bigger values of electric charges and efficiencies by increasing the hairy charge. On the other side, hairy charge causes a new restriction due to negative entropy and therefore physical critical points start from a point with $q_{phys} > 0$. In figure 2.b we fix electric charge and let hairy charge to be change by holding $P_c = 2$, $P_b = 1$, $S_c = 8$, $S_d = 10$. As we can see there is a minimum point at which system has a minimum efficiency and so in this case efficiency behaves more complicated rather than previous case. The green line indicates case of electric charge independent at which (as we discussed before) hairy charge must be have negative value to have physical critical points, so all positive values of h are not physical for this line. Considering this condition the absolute value of maximum hairy charge ($h_{max} = -0.6066$ with $\eta_{max} = 0.553$) and minimum point (with $h_{min} = -0.418$ and $\eta_{min} = 0.476$) both are physical. However for $q \neq 0$, hairy charge could be positive or negative, thus in contrary to the case where $q = 0$, the physical critical points have $h > 0$ provided that they satisfy positive entropy condition. For instance for $q = 0.5$ indicated by blue line, all critical points with $h > 0.8425722021$ are not physical. This diagram shows that by increasing electric charge, both maximum and minimum points are satisfied for smaller hairy charges but

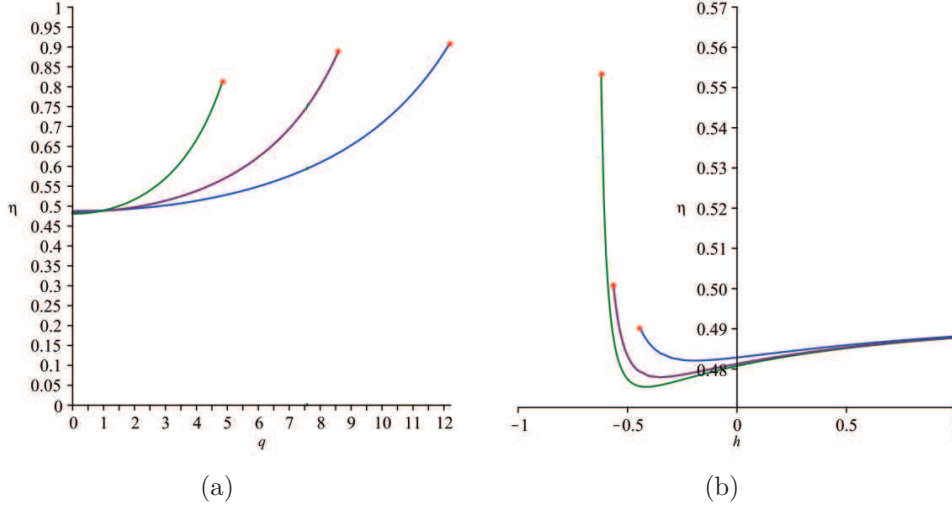


Figure 2: Efficiency is plotted versus the Maxwell electric charge q in (a) and the hairy charge h in (b) by fixing h in (a) and q in (b) respectively. In (a) diagrams reach to a maximum point at $q > 0$ while in (b) they reach to a maximum point at $h < 0$. In (a) Green, purple and blue lines indicate fixed values $h = 0, 0.5$ and 1 respectively for which maximum point is $q_{max} = 4.890, \eta_{max} = 0.824$ for green line, $q_{max} = 8.572, \eta_{max} = 0.885$ for purple line and $q_{max} = 12.234, \eta_{max} = 0.915$ for blue line respectively. In (b) Green, purple and blue lines indicate fixed values $q = 0, 0.25$ and 0.5 , respectively.

with different behavior in their efficiencies. Actually, the maximum point will has smaller efficiency by increasing electric charge while the efficiency grows for the minimum point. Indeed, for fixed large electric charge, their efficiencies reach together.

We can compare the heat engine efficiency η with the Carnot efficiency $\eta_c = 1 - \frac{T_{low}}{T_{high}}$ where T_{low} and T_{high} are the lowest and the highest temperature of the heat engine in cycle under consideration. Diagrams 3.a and 3.b show that when we holed electric (hairy) charge with a constant value, then $\eta_h \rightarrow 1$ at maximum value of hairy (electric) charge. Diagram 3.a shows that for fixed larger q we have smaller absolute value for h_{max} for which $\eta_c \rightarrow 1$, in contrary, 3.b shows that by increasing the hairy charge h we will have bigger q_{max} . There is similar analysis for relations between q and h with physical critical points as we discussed already. The ratio η/η_c is plotted versus the hairy and Maxwell electric charges in figures 4.a and 4.b, respectively. In

figure 4.a with $h = 1$ one can see decreasing of this ratio by increasing the Maxwell charge, while with $q = 1$ in figure 4.b we see inverse behavior for it. One can see that η/η_c increases by raising the hairy charge. For large h it approaches to 1 which means that $\eta \rightarrow \eta_c$.

•*Approaching the Carnot Limit:* As it studied in [56,57] when we put

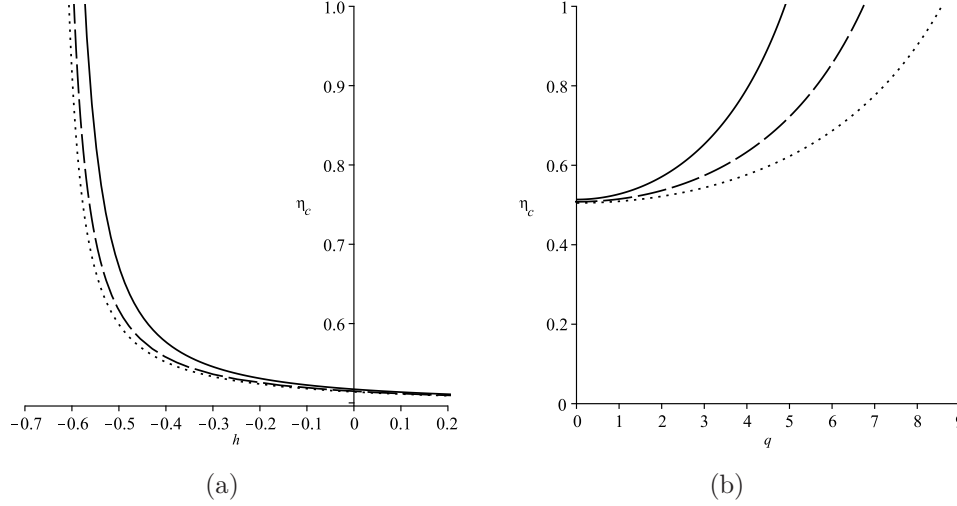


Figure 3: Behavior of the Carnot efficiency is plotted versus the charges for fixed q in (a) and fixed h in (b) respectively. Solid, dash and dotted lines represent $q = 0.5, 0.25, 0$ in (a), and $h = 0, 0.25, 0.5$ in (b) respectively.

one of the corner of rectangular cycle in the critical points of the system or near to them, the efficiency of heat engine could be approached to the Carnot efficiency having the finite power. In [14] we can see good results for charged-AdS black hole in the limit of large charge. Following this work we put the critical point $(P_{\text{cr}}, V_{\text{cr}})$ in corner a and choose the boundary conditions as

$$\begin{aligned}
 P_a = P_b = P_{\text{cr}}, \quad P_c = P_d = \frac{3}{2}P_{\text{cr}}, \\
 V_d = V_a = V_{\text{cr}}, \quad V_b = V_c = V_{\text{cr}}\left(1 - \frac{L}{h^{2/3}}\right),
 \end{aligned}
 \tag{3.10}$$

in which the constant parameter L comes from dimensional analysis. For large values of the charge we can put $\alpha \equiv \frac{L}{h^{2/3}} \rightarrow 0$. The work done by the engine could be simply calculated by the area of $\Delta V \Delta P$ diagram in the cycle

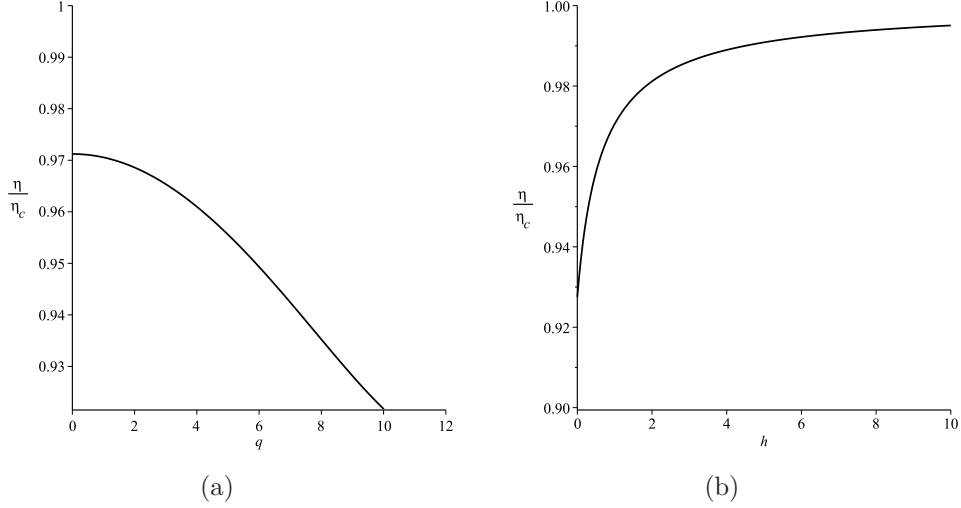


Figure 4: Diagram of ratio η/η_c is plotted versus the charges for $P_c = 2$, $P_b = 1$, $S_c = 8$ and $S_d = 10$ where $h = 1$ in (a) and $q = 1$ in (b).

under consideration as follows.

$$W = \frac{1}{2}P_{\text{cr}}V_{\text{cr}}\alpha = \frac{9 \times 5^{2/3}}{160}\pi L. \quad (3.11)$$

Note that the work done in cycle under the above considerations is finite and independent of hairy charge. The heat absorbed by the system is given by

$$Q_H = M_2 - M_1 = \frac{3\pi}{8}(5H)^{2/3} \left((1-\alpha)^{1/2} + \frac{1}{20}(9\alpha + 24 - 4(1-\alpha)^{-1/4}) \right), \quad (3.12)$$

where by attention to the negativity of hairy charge for black hole system free of Maxwell electric charge we put $H = -h$ as the absolute value of h . For large values of the hairy charge for which $\alpha \rightarrow 0$, the absorbed heat energy by the system takes the following form

$$Q_H = \frac{27\pi}{80}(5H)^{2/3}\alpha + \frac{9\pi}{256}(5H)^{2/3}\alpha^2 + \frac{15\pi}{1024}(5H)^{2/3}\alpha^3 + \mathcal{O}(\alpha^4). \quad (3.13)$$

Therefore, the efficiency of the heat engine (3.9) leads to the following form

$$\eta = \frac{1}{6} \left(1 - \frac{5}{48H^{2/3}} - \frac{25}{768H^{4/3}} + \frac{875}{110592H^2} + \dots \right) \quad (3.14)$$

where we used (3.11) and put $L = 1$. In the other side, the Carnot efficiency as we discussed before depends just on the highest (T_H) and the lowest (T_C) temperatures of the heat engine where they happen at the corners d and b , respectively. In limits of the large hairy charge we obtain

$$T_H = \frac{9}{50\pi} \left(\frac{25}{H}\right)^{1/3}, \quad (3.15)$$

and

$$T_C = \frac{3}{20\pi} \left(\frac{25}{H}\right)^{1/3} - \frac{1}{640\pi} \left(\frac{25}{H^7}\right)^{1/3} + \dots. \quad (3.16)$$

Substituting (3.15) and (3.16) into the definition of the Carnot efficiency one can infer

$$\eta_c = 1 - \frac{T_C}{T_H} = \frac{1}{6} \left(1 + \frac{5}{96H^2} + \dots\right). \quad (3.17)$$

By attention to (3.14) and (3.17) we can conclude $\eta \approx \eta_c$ for large hairy charge $H \rightarrow \infty$ (see figure 5).

By attention to the critical pressure (2.24) we can obtain $P \sim H^{-2/3}$ and so $\tau \sim H^{2/3}$. According to the work [14] one can infer that τ is the necessary time to complete a cycle scales at a finite hairy charge leading to a finite power W/τ in which W is work given by (3.11) (see [57,58]) such that

$$\frac{W}{\tau} \leq \bar{\Theta} \frac{\eta(\eta_c - \eta)}{T_C}. \quad (3.18)$$

In the above equation $\bar{\Theta}$ is a model dependent constant and the right hand side efficiency function would be expanded versus the large hairy charge $H(\equiv -h)$ as follows:

$$\frac{\eta(\eta_c - \eta)}{T_C} = \frac{5^{4/3}\pi}{1296} \left(H^{-1/3} + \frac{5}{24} H^{-1} + \frac{827}{2304} H^{-5/3} + \dots \right). \quad (3.19)$$

When the hairy charge goes to infinity and so $\eta = \eta_c$ then the power (3.18) vanishes as we expect. The universal trade-off relation (3.18) (see [57]) as a bound between power and efficiency would be satisfied for any values of h .

4 Conclusions

As thermodynamics of the black holes with the scalar hair configurations are favored more than of the non-hairy ones, thus we studied thermodynamics

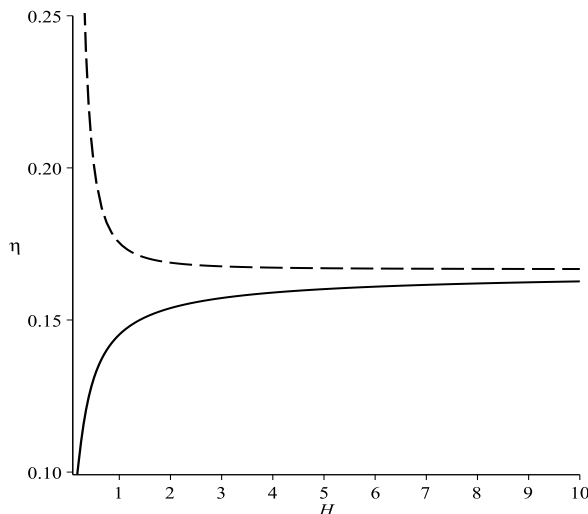


Figure 5: Diagrams of the heat engine efficiency (solid line) and the Carnot efficiency (dash line) are plotted versus the large hairy charge H for a black hole solution with zero Maxwell electric charge $q = 0$.

of black holes in AdS space time which have both electric charge and hairy charge. In the latter case the cosmological constant plays as thermodynamic variable. As the thermodynamic processes of black hole system construct a closed cycle then it operates similar to a heat engine. So we can study this black hole heat engine as an implement of the black hole thermodynamics. We study thermodynamics of the hairy black holes in AdS_5 space-time due to the interesting features of its phase transition. From [53] we know that the Maxwell electric and hairy charges are bounded together and the sign of entropy depends on this bound. Looking to the work [53] we understand that positive critical points are divided into physical and un-physical branches with which represent positive and negative entropies, respectively. We found out from the discussion leading to the figure.2 that for a fixed hairy charge the efficiency of black hole solution (which acts as a heat engine) changes by the Maxwell electric charge. Maximum value of the efficiency is happened at a maximum charge after which we have unacceptable negative temperature. This maximum point moves to larger values by choosing bigger fixed hairy charges. It could be seen from figure (2.a) the blue line has the biggest value of fixed h and so it has biggest maximum points for the Maxwell charge and efficiency. Indeed for bigger Maxwell charges in these diagrams the system

enters to an un-physical situation which is not acceptable. In the other side, we found also a minimum value of the efficiency in the case of fixed electric charge which could be seen in figure (2.b) graphically. We concluded that if we choose $q = 0$ then all critical points for $h > 0$ will be un-physical, however for all other fixed $q \neq 0$ we have physical critical points with positive hairy charges for which the entropy remains positive. Maximum and minimum critical values are physical for all values of fixed electric charges and they have different behavior by increasing the Maxwell electric charge. By increasing q , maximum (minimum) point happens at smaller hairy charges but with smaller(larger) efficiency. It means for example if we choose larger values for a fixed Maxwell electric charge then the hairy charge for both maximum and minimum point decreases, but we can see this change make the value of efficiency smaller(larger) for the maximum(minimum) point. We also compared this efficiency with Carnot efficiency and conclude that the ratio η/η_c will decrease by changing of Maxwell charge when $h = \text{constant}$. On the other side when we choose a fixed hairy charge it could be seen that $\eta \rightarrow \eta_c$ for large h . Regarding [14] and by putting one corner of rectangular cycle of heat engine process on or near critical points of the system the efficiency of heat engine reaches to the Carnot efficiency having a finite power. We studied it in large hairy charge limit when the power vanishes.

Previously, thermodynamic processes were studied for various black hole systems as heat engines, but by considering a conformal scalar hair arising from coupling of a real scalar field with dimensionally extended Euler densities, can help us to explore more profound in thermodynamic behavior of black holes. Considering the hairy charge could be also important when we try to found out its behavior in field theory side in AdS/CFT proposal. It could be correspond to some kind of hyper charges or baryon numbers. As the black hole has scalar hair it could be make contact with something more akin to a superconducting phase like which we can explore in [59] and [60].

5 Acknowledgment

We would like to thank the editor Prof. *Stephan Stieberger* and anonymous reviewers for their valuable guidance and also *Pavan Kumar Yerra* from *Indian Institute of Technology Bhubaneswar* for our discussions and his useful comments which caused to improve the work.

References

1. J. D. Bekenstein, "Black holes and entropy." *Phys. Rev. D* 7, 2333, (1973).
2. S. W. Hawking, "Particle creation by black holes." *Commun. Math. Phys.* 43, 199, (1975).
3. S. W. Hawking and P. Don "Thermodynamics of black holes in anti-de Sitter space", *Commun. Math. Phys.* 87, 577, (1983).
4. A. Chamblin, R. Emparan, C. V. Johnson and R. C. Myers "Charged AdS black holes and catastrophic holography." *Phys. Rev. D* 60, 064018, (1999).
5. A. Chamblin, R. Emparan, C. V. Johnson and R. C. Myers. "Holography, thermodynamics, and fluctuations of charged AdS black holes." *Phys. Rev. D* 60, 104026, (1999).
6. L. Smarr, "Mass Formula for Kerr BlackHoles", *Phys. Rev. Lett* 3, 71 (1972), Erratum *ibid.*, 30, 521 (1973).
7. S.Q. Hu, X.M. Kuang and Y.C. Ong, "A Note on Smarr Relation and Coupling Constants" ,*Gen. Relativ. Gravit.* 51, 55 (2019), gr-qc/1810.06073
8. M. M. Caldarelli, G. Cognola, and D. Klemm. "Thermodynamics of Kerr-Newman-AdS black holes and conformal field theories." *Class. Quant. Grav.* 17, 399, (2000).
9. D. Kastor, S. Ray and J. Traschen "Enthalpy and the mechanics of AdS black holes." *Class. Quant. Grav.* 26, 195011, (2009).
10. L. Girardello, M. Petrini, M. Porrati, and A. Zaffaroni. "Novel local CFT and exact results on perturbations of N=4 super Yang Mills from AdS dynamics." *JHEP* 1998, 022, (1999).
11. J. Distler and F. Zamora. "Non-supersymmetric conformal field theories from stable anti-de Sitter spaces", *Adv. Theor. Math. Phys.* 2, 1405, (1999), hep-th/9810206.
12. C. V. Johnson "Holographic heat engines." *Class. Quant. Grav.* 31, 205002, (2014).

13. C. V. Johnson, "An exact efficiency formula for holographic heat engines" *Entropy* 18, 120, (2016).
14. C. V. Johnson and F. Rosso. "Holographic heat engines, entanglement entropy, and renormalization group flow." *Class.Quant.Grav.* 36, 015019 (2019), hep-th/1806.05170.
15. C. V. Johnson "An Exact model of the power-to-efficiency trade-off while approaching the Carnot limit." *Phys. Rev. D* 98, 026008, (2018).
16. C. V. Johnson, "Gauss-Bonnet black holes and holographic heat engines beyond large N ." *Class. Quant. Grav.* 33, 215009, (2016).
17. C. V. Johnson, "BornInfeld AdS black holes as heat engines." *Class. Quant. Grav.* 33, 135001, (2016).
18. A. Belhaj, M. Chabab, H. El Moumni, K. Masmar, M. B. Sedra and A. Segui. "On heat properties of AdS black holes in higher dimensions." *JHEP* 2015, 149, (2015).
19. B. Chandrasekhar and P. K. Yerra. "Heat engines for dilatonic BornInfeld black holes." *Eur. Phys. J. C* 77, 534, (2017).
20. A. Chakraborty and C. V. Johnson, Benchmarking Black Hole Heat Engines,, *Int. J. Mod. Phys. D*28, 1950012 (2019), hep-th/1612.09272.
21. A. Chakraborty and C. V. Johnson. "Benchmarking Black Hole Heat Engines, II", *Int. J. Mod. Phys. D*28, 1950006 (2019), hep-th/1709.00088.
22. R. A. Hennigar, F. McCarthy, A. Ballon and R. B. Mann. "Holographic heat engines: general considerations and rotating black holes." *Class. Quant. Grav.* 34, 175005, (2017).
23. C. V. Johnson, "Taub-Bolt heat engines." *Class. Quant. Grav.* 35, 045001, (2018).
24. H. Liu, and X. H. Meng. "Effects of dark energy on the efficiency of charged AdS black holes as heat engines." *Eur. Phys. J. C* 77, 556, (2017).
25. J. X. Mo and G. Q. Li "Holographic heat engine within the framework of massive gravity." *JHEP* 122, (2018).

26. S. H. Hendi, B. E. Panah, S. Panahiyan, H. Liu, and X. H. Meng. "Black holes in massive gravity as heat engines." *Phys. Lett. B* 781, 40, (2018).
27. S. W. Wen, and Y. X. Liu. "Charged AdS black hole heat engines." *Nucl. Phys. B* 946, 114700 (2019) gr-qc/1708.08176.
28. F. Rosso, "Holographic heat engines and static black holes: a general efficiency formula", *Int.J.Mod.Phys. D*28 (2019), hep-th/1801.07425.
29. J. X. Mo and S. Q. Lan. "Phase transition and heat engine efficiency of phantom AdS black holes" *Eur. Phys. J. C*78, 666 (2018), gr-qc/1803.02491.
30. N. Bocharova, K. Bronnikov, and V. Melnikov, "An exact solution of the system of Einstein equations and mass-free scalar field", *Vestn. Mosk. Univ. Fiz. Astronom.* 6, 706 (1970)
31. B. C. Xanthopoulos and T.E. Dialynas, "Einstein gravity coupled to a massless conformal scalar field in arbitrary space time dimensions." *J. Math. phys.*33, 1463, (1992).
32. J. D. Bekenstein, "Black holes with scalar charge", *Ann. Phys. (N.Y.)* 91, 75, (1975).
33. R. G. Cai, L. M. Cao, L. Li, and R. Q. Yang. "PV criticality in the extended phase space of Gauss-Bonnet black holes in AdS space." *JHEP* 2013, 5, (2013).
34. C. Klimcik, "Search for the conformal scalar hair at arbitrary D" *J. Math. phys.* 34, 1914, (1993).
35. C. Martinez and J. Zanelli, "Conformally dressed black hole in 2+ 1 dimensions." *Phys. Rev. D* 54, 3830, (1996).
36. C. Martinez, J. P. Staforelli and R. Troncoso, "Topological black holes dressed with a conformally coupled scalar field and electric charge." *Phys. Rev. D* 74, 044028 (2006).
37. C. Martinez, R. Troncoso, and J. Zanelli. "de Sitter black hole with a conformally coupled scalar field in four dimensions." *Phys. Rev. D* 67, 024008 (2003).

38. A. Anabalon and H. Maeda, "New charged black holes with conformal scalar hair." *Phys. Rev. D* 81, 041501 (2010).
39. S. Bhattacharya and H. Maeda. "Can a black hole with conformal scalar hair rotate?." *Phys. Rev. D* 89, 087501 (2014).
40. C. Martinez, "*In Quantum Mechanics of Fundamental Systems: The Quest for Beauty and Simplicity*", edited by M. Henneaux and J. Zanelli (Springer, New York, 2009).
41. F. Oliva, and S. Ray, "Conformal couplings of a scalar field to higher curvature terms." *Class. Quant. Grav.* 29, 205008 (2012).
42. G. Giribet, M. Leoni, J. Oliva and S. Ray, "Hairy black holes sourced by a conformally coupled scalar field in D dimensions." *Phys. Rev. D* 89, 085040 (2014).
43. M. Chernicoff, M. Galante, G. Giribet, A. Goya, M. Leoni, J. Oliva, and G. P. Nadal, "Black hole thermodynamics, conformal couplings, and R^2 terms," *JHEP* 2016, 159, (2016).
44. G. Giribet, A. Goya and J. Oliva. "Different phases of hairy black holes in AdS 5 space." *Phys. Rev. D* 91, 045031 (2015).
45. K. Bamba, "Thermodynamic properties of modified gravity theories." *Int. J. Geomet. Meth. Mod. Phys.* 13, 06, 1630007, (2016); gr-qc/1604.02632.
46. S. Nojiri, and S. D. Odintsov, "Unified cosmic history in modified gravity: from $F(R)$ theory to Lorentz non-invariant models." *Phys. Rep.* 505, 59, (2011).
47. S. Capozziello and M. De Laurentis, "Extended theories of gravity." *Phys. Rep.* 509, 167, (2011).
48. S. Nojiri, S. D. Odintsov, and V. K. Oikonomou. "Modified gravity theories on a nutshell: inflation, bounce and late-time evolution." *Phys. Rep.* 692 1, (2017).
49. S. Capozziello, and V. Faraoni. *Beyond Einstein gravity: A Survey of gravitational theories for cosmology and astrophysics*. Vol. 170. Springer Science and Business Media, (2010).

- 50. K. Bamba, and S. D. Odintsov. "Inflationary cosmology in modified gravity theories." *Symmetry* 7, 220, (2015); hep-th/1503.00442.
- 51. K. Bamba, S. Capozziello, S. Nojiri, and S. D. Odintsov, "Dark energy cosmology: the equivalent description via different theoretical models and cosmography tests." *Astrophys. and Space Sci.* 342, 155, (2012).
- 52. R. Hennigar and R. Mann. "Reentrant phase transitions and van der Waals behavior for hairy black holes." *Entropy* 17, 8056, (2015).
- 53. D. Kubiznak and R. B. Mann, P-V criticality of charged AdS black holes, *JHEP* 1207, 033, (2012).
- 54. J. D. Bekenstein, "Exact solutions of Einstein-conformal scalar equations", *Ann. Phys. (N.Y.)*82, 535 (1974)
- 55. M. Polettini, G. Verley and M. Esposito "Efficiency statistics at all times: Carnot limit at finite power." *Phys. Rev. Lett.* 114, 050601, (2015).
- 56. M. Campisi and R. Fazio. "The power of a critical heat engine." *Nat. Commun.* 7, 11895, (2016).
- 57. N. Shiraishi, K. Saito and H. Tasaki, "Universal trade-off relation between power and efficiency for heat engines." *Phys. Rev. Lett.* 117, 190601, (2016).
- 58. N. Shiraishi and H. Tajima. "Efficiency versus speed in quantum heat engines: Rigorous constraint from Lieb-Robinson bound." *Phys. Rev. E* 96, 022138, (2017).
- 59. S. A. Hartnoll, P. H. Christopher and G. T. Horowitz, "Holographic superconductors." *JHEP* 2008, 015, (2008), hep-th/0810.1563.
- 60. S. S. Gubser, "Colorful Horizons with Charge in Anti-de Sitter Space." *Phys. Rev. Lett.* 101, 191601, (2008), hep-th/0803.3483.